European Review for Medical and Pharmacological Sciences 2020; 24: 12423-12436

Novel peptidic dual GLP-1/glucagon receptor agonist alleviates diabetes and diabetic complications in combination with low-intensity ultrasound

W.-X. DING[1], H.-Y. WANG[2], L.-J. PENG[3], F. ZHANG[4], S. YUAN[1], L.-H. ZHAO[5]

[1]The First Affiliated Hospital, Zhejiang University, Hangzhou, Zhejiang Province, China
[2]College of the Second Clinical Medical, Zhejiang Chinese Medical University, Hangzhou, Zhejiang Province, China
[3]College of Pharmaceutical Sciences, Zhejiang University, Hangzhou, Zhejiang Province, China
[4]College of the First Clinical Medical, Zhejiang Chinese Medical University, Hangzhou, Zhejiang Province, China
[5]Women's Hospital School of Medicine, Zhejiang University, Hangzhou, Zhejiang Province, China

Abstract. – OBJECTIVE: To design and evaluate a novel oxyntomodulin (OXM) derivative with albumin-binding helix domain and dual GLP-1 receptor (GLP-1R) and glucagon receptor (GcgR) activation activity to achieve metabolize improvement on the diabetes-related complication.

MATERIALS AND METHODS: Mutation (D-Ser2) on OXM was performed and then different helix albumin-binding domains were fused to the mutated OXM *via* a thrombin-cleavable linker to generate seven fusion peptides, named LM01-LM07. Seven LM peptides were synthesized and screened *via in vitro* receptor activation test, albumin binding measurement and protease cleavage assay to select potent candidate peptide for further in vivo study. Moreover, acute and chronic efficacy studies were conducted to evaluate the efficacy of selected candidate using db/db mice.

RESULTS: LM06, as selected OXM derivative, exhibited higher albumin-binding affinity, sustained-release efficiency and balanced activation activities on both GLP-1R and GcgR compared with other ones. Moreover, LM06 was demonstrated with improved hypoglycemic and insulinotropic abilities in receptor-deficient mice via activating GLP-1R. In addition, prolonged anti-diabetic efficacies of LM06 were demonstrated *via* hypoglycemic duration assay and OGTT in db/db mice. Further pharmacokinetic test of LM06 in both rats and monkeys identified improved half-life and other metabolic characteristics. Nevertheless, 8-week subcutaneously dosed LM06 in db/db mice achieved prominent efficacies on glucostasis, weight-lowering, pancreatic function and adipogenesis *via* activating GLP-1R and GcgR. Moreover, LM06 also could accelerate diabetic skin wound closure in combination with low-intensity ultrasound.

CONCLUSIONS: LM06, as a long-acting dual GLP-1R/GcgR agonist, exerts potential as a once-weekly therapeutic candidate against diabetes-related complication in combination with low-intensity ultrasound.

Key Words:
GLP-1, Glucagon, Oxyntomodulin, Helix, Albumin, Obesity, Diabetes.

Introduction

Diabetes, especially for type 2 diabetes mellitus (T2DM), is a metabolic disorder characterized by hyperglycemia and gradual worsening insulin resistance[1,2]. Usually, the increasing incidence and prevalence of T2DM are associated with increasing obesity[3-5]. To date, the treatment of "diabesity" (the co-existence of T2DM and obesity) has focused on dietary strategies or pharmacological treatments[6]. However, the long-term complex dietary interventions, such as reducing energy intake or improving diet quality, suffer from limited efficacy because of the low dietary compliance[7,8]. However, the current pharmaceuticals for T2DM are limited with adverse effects and unsatisfied body weight control[4,9,10]. Therefore, many efforts have been devoted to developing the antidiabetic agent with simultaneous effect in glycemic and body weight control.

Corresponding Author: Wenxiu Ding, MD; e-mail: wxding@ncstmc.cn

OXM is a kind of the peptide hormones with a 37-amino acids and homologous sequence to GLP-1, as well as glucagon[11,12]. OXM has been demonstrated as a natural dual agonist for GLP-1R and GcgR with ability to increase energy expenditure and regulate glucose metabolism[12,13]. Natural OXM has emerged as an attractive therapeutic agent for the treatment of diabetes and obesity due to its advantageous properties of achieving both glycemic control and weight loss[14,15]. Nevertheless, the clinical effectiveness of OXM is currently limited due to the susceptibility to dipeptidylpeptidase-IV (DPP-IV) degradation[14]. Therefore, engineering OXM is currently underway to avoid protease digestion and rapid glomerular filtration so to enhance the *in vivo* circulatory half-life[14].

Currently, human serum albumin (HSA) has been wildly used as a carrier to protect small polypeptide from *in vivo* enzymatic degradation, as well as glomerular filtration due to its inherent long blood circulation[16,17]. We previously reported the design and evaluation of a novel HSA-binding domain which showed promising affinity for HSA within femtomolar level[18]. In general, a natural 46-residue three-helix bundle domain with nanomolar affinity for HSA was used as a template, and further strategy of combinatorial protein-engineering was applied to design the variants based on the targeted fifteen residues showing enhanced HSA-binding affinity[18]. These peptidic helix variants, such as GI48-ABD, exhibited similar secondary structure with wild type one and showed HSA affinity within the range of 50-500 fM[18].

In this study, we fused a modified OXM analog to different helix domains via a thrombin-cleavable site (FNKP) to generate a series of OXM derivatives. Furthermore, the *in vitro* albumin binding test and protease cleavage assay, as well as dual receptor activation were further evaluated to confirm the optimal OXM derivative. As a proof of concept study, both *in vivo* efficacies and pharmacokinetic parameters of selected OXM derivative were performed in this study.

Materials and Methods

Materials and Animals

The positive control, Semaglutide, was obtained from Novo Nordisk (Copenhagen, Denmark). Male C57BL/6J, GLP-1R$^{-/-}$, GcgR$^{-/-}$, db/db mice, SD rats and cynomolgus monkey were purchased from Zhejiang Experimental Animal Center. All animals were housed in the animal facility with groups of 6 mice, 3 rats and 1 monkey per cage, respectively. All animals maintained on a standard 12-hour light/dark cycle with free access to food and water. All the animal experimental procedures were conducted in accordance with guideline and approved by Center for Experimental Animal Ethics of Zhejiang University.

Preparation of Novel OXM Analogs

All OXM derivatives were produced by using the traditional solid phase synthesis method. Briefly, Fmoc protected amino acid (5 equvi) were pre-activated with HBTU (4.9 equvi), HOBt (5.0 equvi) and DIPEA (10.0 equvi) in DMF. The resin was washed with DMF and monitored by using the qualitative ninhydrin test. Subsequently, the peptides were dissolved again in 0.1 % TFA followed by purification with reversed-phase high-performance liquid chromatography (RP-HPLC).

In Vitro Activation Test

CHO cell stably expressing GcgR and GLP-1R were applied to determine *in vitro* potency of OXM derivatives. The GLP-1R or GIPR activations of these derivatives were assessed by measuring the Luciferase expression according to previously reported method[19]. The values of the EC_{50} were calculated by using GraphPad Prism 6 (San Diego, CA, USA).

Surface Plasmon Resonance (SPR) Measurement

The HSA-binding affinities of seven OXM derivatives were performed by using SPR method. Firstly, the HSA proteins were covalently coated on surface of microsensor chip to obtain the final response values at the level of ~3000 RU. Subsequently, 40 **μ**L of OXM derivatives (100 **μ**g/mL) in buffer were loaded on the surface of the microsensor chip which was coated with the HSA (flow rate: 5 μL/min) for the further association experiment. The association and dissociation rate constants (ka, kd) were calculated by BIA evaluation software (version 3).

In Vitro Protease Cleavage Test

The protease cleavage test was carried out in monkey serum with OXM derivatives and thrombin at final concentrations of 1 mg/L and 0.4 U/mL, respectively. Subsequently, the reaction

mixtures were statically put at 37°C in the dark for 72 hours. The released OXM and different hydrolysed fragments were detected at the time point of 12 and 72 h by using LC-MS/MS method according to previously reported details[20].

Oral Glucose Tolerance Test in db/db Mice

After 15-hour fasting, 6-8 weeks old male wild-type (WT), GLP-1R$^{-/-}$ and GcgR$^{-/-}$ mouse was subcutaneously (s.c.) injected of LM06 at the single dose of 50, 100 and 200 nmol/kg half an hour before oral glucose loading at the dose of 2 g/kg. The blood glucose levels (BGLs) of the samples from mouse tails were measured at indicated time points of 0, 15, 30, 45, 60 and 120 min by using a glucometer. The serum level of insulin was measured by using commercial ELISA kit (Abcam, Cambridge, MA, USA). The multiple OGTTs were further conducted to assess the ability of LM06 to consistently control BGL in the diabetic db/db mice. The oral glucose loading was performed at 0, 72 and 144 h after single dose injection of LM06 at the doses of 50, 100 and 200 nmol/kg and the measurement of BGLs were performed as above mentioned.

Hypoglycemic Duration Test in Diabetic Mice

The diabetic mice were subcutaneously administrated with a single injection of placebo, LM06 at the doses of 50, 100 and 200 nmol/kg, as well as Semaglutide at the dose of 200 nmol/kg. The blood samples from mouse tail vein were measured at the time points of 0, 1, 2, 4, 8, 12, 24, 36, 48, 72, 96 and 120 h as the method described above.

Pharmacokinetics Tests

The pharmacokinetics tests of LM06 at 50, 100 and 200 nmol/kg were performed in SD rats and cynomolgus monkeys. The serum sample of SD rats and monkeys were collected at the time points of 0, 4, 8, 12, 24, 36, 48, 72, 96, 120, 144 and 168 h from the tails of SD rats and right fore of monkeys, respectively, and the serum concentration of LM06 were measured by using the method of the LC-MS/MS according to previously reported details.

Chronic Study in db/db Mice

The db/db mice were treated with Semaglutide (200 nmol/kg) and LM06 (50, 100 and 200 nmol/kg) twice a week for consecutive 8 weeks. The body weight gain and food intake of diabetic mice were recorded daily. The ^{13}C-labelled octanoic acid breath test, insulin resistance test (ITT) and OGTT were carried out to evaluate the gastric emptying changes, insulin tolerance and glucose tolerance of db/db mice before and after the chronic treatment according to previously reported procedures[21,22]. Furthermore, the whole fat and lean masses were detected using a BCA-body composition analyzer (Bruker, Germany) according to the standard operating instruction.

The blood samples were collected via cheek puncture and separated into two parts at the beginning and end of chronic experiment. One part was mixed with 3.8% sodium citrate anticoagulant to detect the % HbA1c value immediately. The other part was centrifuged at 5000 rpm for 10 min, and the serum samples were collected to measure the levels of LDL, HDL, TC and TG via using ELISA kits (Thermo Fisher Scientific, Waltham, MA, USA). Islet morphology and white adipose tissue (WAT) macrophage infiltration were visualized using a Fluoview F1000 microscope (Olympus, Japan) according to the previously reported method[23].

After the ten weeks old db/db mice were anesthetized, the highest point sites on the back were shaved and disinfected. Then, a circular wound (1 cm) on the back was performed with sterile scissor and forceps. Then, the model mice were divided into four groups: negative control group, LM06 (200 nmol/kg), low-intensity ultrasound group, and LM06+low-intensity ultrasound group. In present study, CZ-960 pulsed ultrasonic cavitation therapeutic apparatus was used to irradiate the wound with 4.6 MPa acoustic pressure at the body surface marker. The irradiation time was 10 min, the pulse width was 1.2 ms, the duty cycle was 1%, and the working/intermittent time was 5s/5s. Each mouse was single-housed and observed daily for wound changes to assess the wound healing process.

Statistical Analysis

All the data were analyzed via using GraphPad Prism 6 (San Diego, CA, USA). Differences between groups were determined using one-way ANOVA. p-value of 0.05 or less was considered significant.

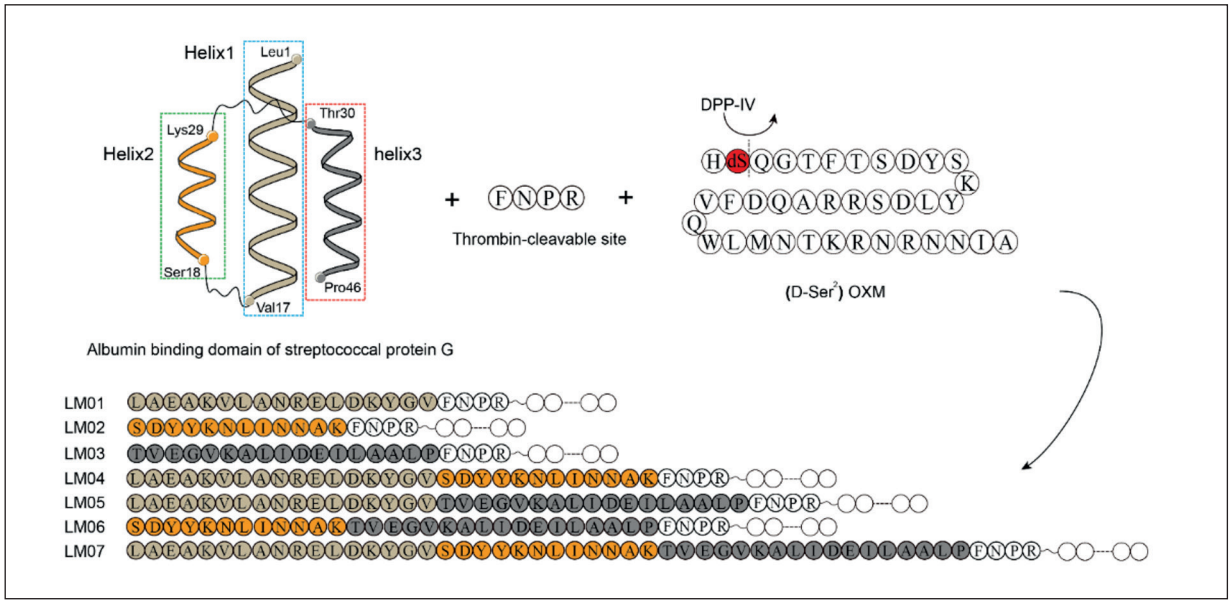

Figure 1. Design and schematic structures of LM peptides.

Results

Design, Preparation and Identification of Long-Acting OXM Analogs

According to the previous reports[24], D-serine substitution at position 2 of OXM could completely inhibit the *in vivo* DPP-IV degradation. Therefore, we utilized D-Ser^2-OXM as a bioactive peptide for subsequent structure-based optimization for balanced receptor activation and control-release. As shown in Figure 1, seven OXM derivatives, termed LM01-LM07, were designed by fusing different helixes of G148-ABD to the N-terminus of D-Ser^2-OXM via a thrombin-cleavable site (FNKP), which was selected by our previous study[25]. These seven fusion OXM derivatives were synthesized using solid-phase synthesis method with the purities were all over 98%.

Subsequently, *in vitro* receptor activation tests were performed to assess the potencies of LM01-LM07 in CHO cells expressing GcgR or GLP-1R. As results showed in Table I, LM01-LM04 and LM06 all retained the similar activation potency for GLP-1R and GcgR as native OXM. Compared with other ones, the activation potencies of LM05 and LM07 for both receptors were significantly decreased demonstrating that steric hindrance

Table I. Receptor activation of LM peptides for GLP-1R and GcgR.

Peptides	GLP-1R		GcgR	
	EC_{50} (nM)	Relative (%)	EC_{50} (nM)	Relative (%)
GLP-1	0.341	100	> 100	0
Gcg	2.364	14	0.084	100
OXM	0.428	80	0.233	79
D-Ser2-OXM	0.371	92	0.199	81
LM01	0.437	78	0.158	86
LM02	0.404	84	0.287	76
LM03	0.371	93	0.128	90
LM04	0.592	75	0.232	78
LM05	1.234	51	0.465	63
LM06	0.352	97	0.111	93
LM07	1.835	31	0.671	39

Table II. The binding affinity of LM peptides for HSA.

Peptides	ka ($M^{-1}s^{-1}$)	kd (s^{-1})	KD (M)
LM01	1.34×10^{5}	6.93×10^{-4}	5.17×10^{-9}
LM02	6.37×10^{5}	5.96×10^{-4}	9.36×10^{-10}
LM03	4.86×10^{4}	3.71×10^{-4}	7.63×10^{-10}
LM04	2.04×10^{5}	8.27×10^{-4}	4.05×10^{-9}
LM06	7.99×10^{5}	1.22×10^{-4}	1.53×10^{-10}

effects induced by the excessively complex helical structure may affect the binding-affinities for GcgR and GLP-1R. Hence, these five OXM derivatives were selected to conduct further albumin binding affinity test.

Albumin Binding Affinity of LM Peptides

Binding affinities of LM01-LM04 and LM06 for HSA were assessed. As the results showed in Table II, the KD values of LM01-LM04 and LM06 were 5.17×10^{-9}, 9.36×10^{-10}, 7.63×10^{-10}, 1.49×10^{-9}, 4.05×10^{-9} and 1.53×10^{-10} M, respectively, and those ones contained helix 2 or helix 3 or both held the higher binding affinities for albumin. Especially, the attachment of both helix 2 and helix 3 to N-terminus D-Ser^2-OXM showed the highest HSA-binding potency than that of other ones. These results suggested that helix 2 and helix 3 were the effective HSA-binding regions of G148-ABD. Considering the higher HSA-binding affinities compared with other ones, LM02, LM03 and LM06 were selected to perform further *in vitro* evaluation of sustained release profiles.

Protease Cleavage Assay of LM Peptide

To confirm whether the thrombin can stably digest and then slowly release the D-Ser^2-OXM from LM peptides, we performed the thrombin cleavage assays of LM02, LM03 and LM06 in monkey serum. The intact LM peptides, helix-thrombin cleavable site, and released D-Ser^2-OXM in the cleavage reaction mixtures were identified and quantified using LC-MS/MS method, respectively, at 12 h and 72 h (Figure 2A-F). Further calculated results were shown in Figure 2G, the D-Ser^2-OXM were slowly released from

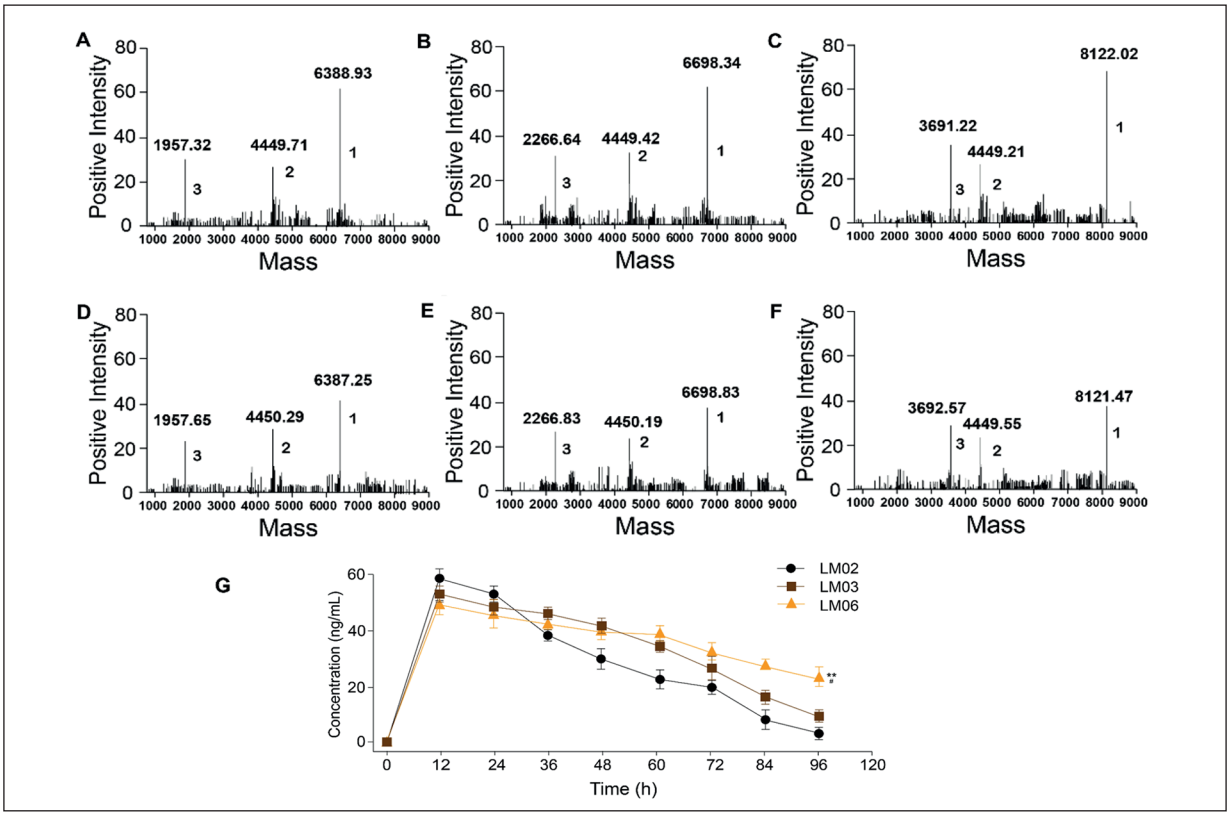

Figure 2. *In vitro* slowly releasing of OXM from novel LM peptides. The mass spectrum showed the hydrolysis of LM02 at 12 h (**A**) and 72 h (**D**), LM03 at 12 h (**B**) and 72 h (**E**), and LM06 at 12 h (**C**) and 72 h (**F**) by thrombin in monkey serum. **G**, Transient concentration of released OXM-time curve. Peak 1, 2 and 3 refer to LM peptide, helix-thrombin cleavable site and released OXM, respectively. $^{**}p<0.01$ *vs.* LM02 group, $^{\#}p<0.05$ *vs.* LM03 group. All above data are shown as means ± SD, n=6.

LM02, LM03 and LM06 via thrombin cleavage and sustained for at least 84 h. Importantly, the concentration of released D-Ser^2-OXM in LM06 group maintained ~30 ng/mL at the time point of 96 h which was significantly higher than that of LM02 or LM03, even than those of the LM02 and LM03 at 84 h, indicating a potent sustainable-released model for treating diabetes and obesity.

Glucose Tolerance and Insulin Secretion Test

Glucose tolerance and insulin secretion tests of LM06 at three doses were performed in WT and GLP-1R or GcgR deficient mice using Semaglutide as positive control. As shown in Figure 3A, the $AUC_{0\text{-}120\ min}$ of plasma insulin level was dose-dependently increased to 8.34±1.94, 13.49±**2**.23 and 19.37±**3**.54 ng/mL.min in WT mice treated with the 50, 100 and 200 nmol/kg of LM06, respectively, while that in the placebo treated group was only 5.04±1.60 ng/mL.min. Meanwhile, increased insulin level attributed to significant reductions on $AUC_{0\text{-}120\ min}$ of BGLs in all LM06 or Semaglutide treated four groups. However, acute treatment of LM06 at the dose of 50 nmol/kg exhibited no evident effect on BGLs in GLP-1R$^{-/-}$ mice, but the significantly increased BGLs were showed in the groups treated with LM06 (100 and 200 nmol/kg) suggesting that GcgR activation will finally increase the BGL due to the blockade of GLP-1R function, while Semaglutide treatment did not affect the BGL. In GcgR$^{-/-}$ mice, LM06 treatment caused a similar insulin level increase and glucose level reduction as those in the WT mice. All these results definitively demonstrated the activation activities of LM06 on both GLP-1R and GcgR.

Multiple Oral Glucose Tolerance Tests

We further accessed *in vivo* hyperglycemic duration of LM06 at the doses of 50, 100 and 200 nmol/kg using multiple OGTTs in the 15-hour fasted db/db mice. As the results showed in Figure 4, the BGLs of db/db mice in negative control group maintained at higher than those of the LM06 or Semaglutide groups throughout the whole experimental period (0-146 h) indicating impaired glucose tolerance induced by insulin resistance in diabetic db/db mice. In contrast, single dose treatment of LM06 at 50, 100 and

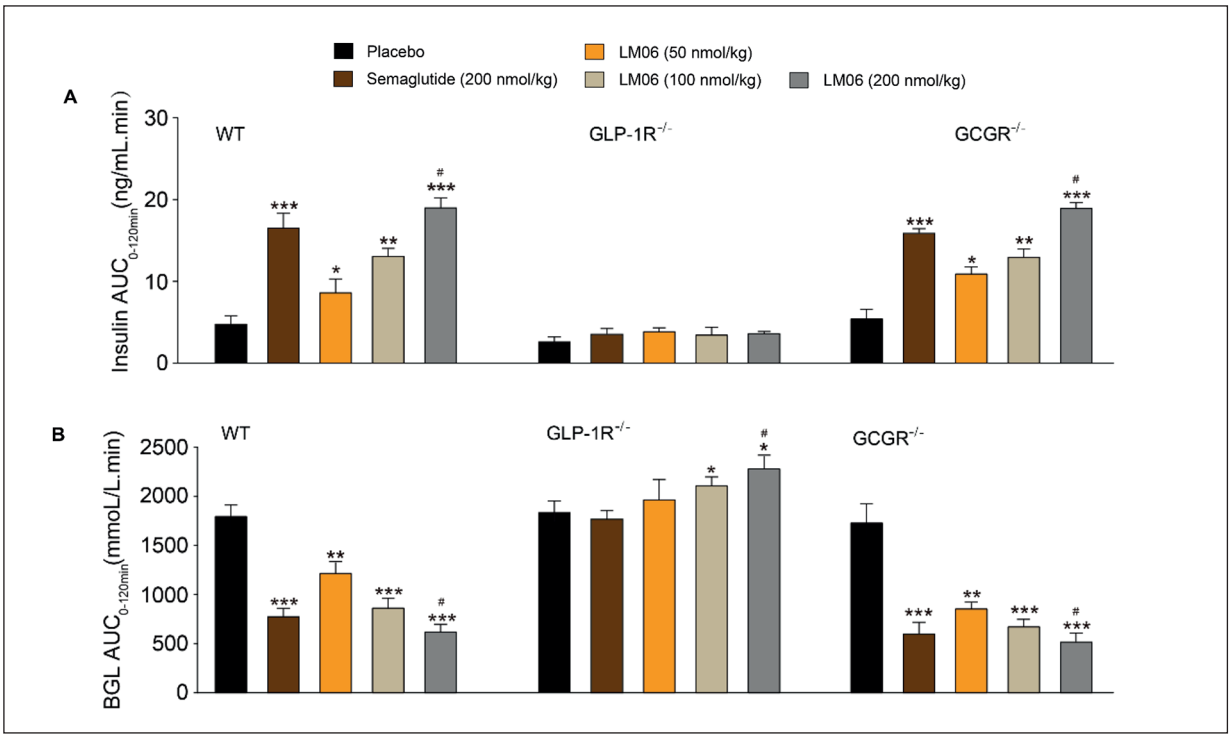

Figure 3. Glucose tolerance test and insulin secretion test of LM06 in WT and receptor deficient mice. The aera under the curve ($AUC_{0\text{-}120\ min}$) of (**A**) insulin levels and (**B**) blood glucose levels of WT, GLP-1R$^{-/-}$ and GcgR$^{-/-}$ mice treated with placebo, LM06 at three doses of 50, 100 and 200 nmol/kg and Semaglutide at 200 nmol/kg. *p<0.05, **p<0.01, ***p<0.001 *vs.* placebo treated ones, $^{\#}p$<0.05 vs. positive control treated ones. All above data shown as means ± SD, n=8.

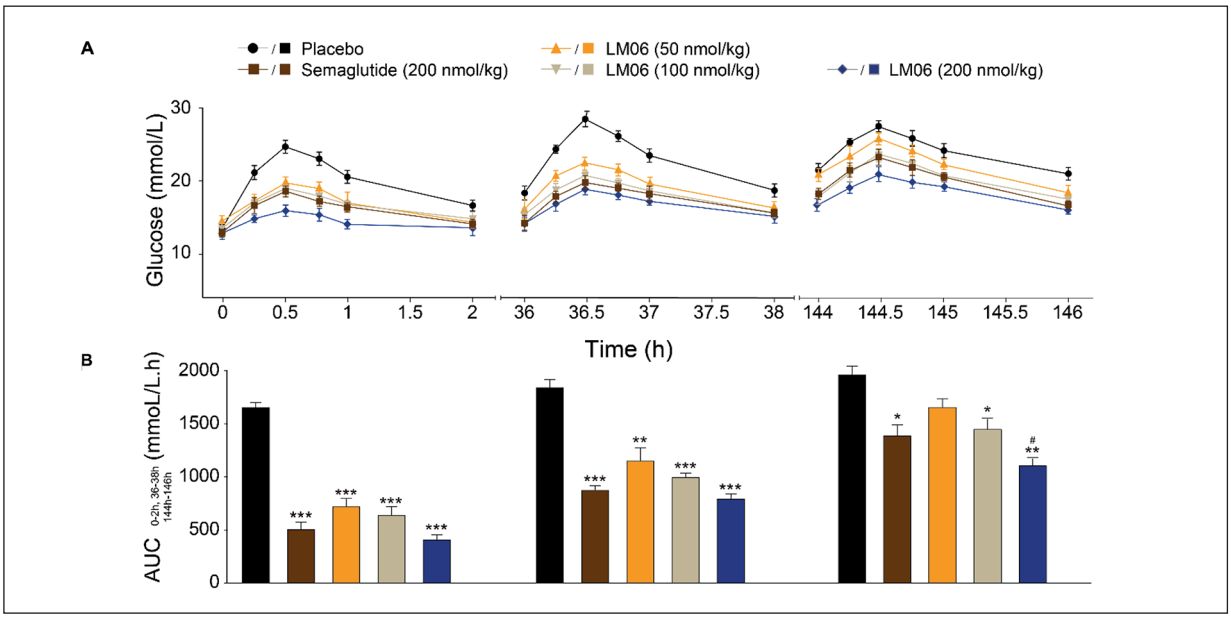

Figure 4. Multiple OGTTs of LM06 in diabetic mice. The (**A**) BGL-time curves and (**B**) $AUC_{0\text{-}120\,min}$ of All above data shown as means ± SD, n=8. *p<0.05, **p<0.01, ***p<0.001 vs. saline group, $^{\#}p$<0.05 *vs.* Semaglutide group.

200 nmol/kg dose-dependently reduce the BGLs of diabetic mice in all three rounds of OGTTs. Interestingly, acute treatment of LM06 at 200 nmol/kg in db/db mice induced a significant reduction on $AUC_{0\text{-}120min}$ value of the third round OGTT compared to that of the Semaglutide treated mice at the same dose (p<0.05) suggesting that LM06 holds enhanced glucoregulatory effect and prolonged hypoglycemic duration than Semaglutide, one of currently best incretin-based antidiabetic drugs.

Hypoglycemic Duration Test

Hypoglycemic duration of LM06 at three doses of 50, 100 and 200 nmol/kg were assessed in the non-fasted diabetic db mice. As the results showed in Figure 5A, the placebo-treated diabetic mice showed a fast hyperglycemia of which the BGL was higher than 20 mmol/L during entire experimental duration. On the contrary, acute treatment of LM06 effectively decreased the postprandial BGL of the diabetic db/db mice. Moreover, the duration of BGL be-

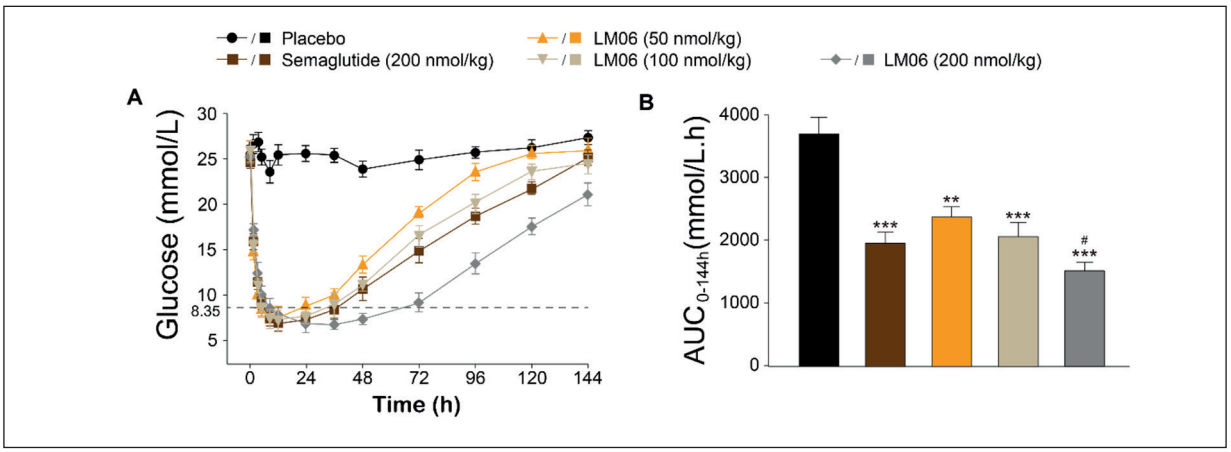

Figure 5. Hypoglycemic duration test of LM06 in diabetic mice. (**A**) The BGL-time curve and (**B**) $AUC_{0\text{-}144\,h}$ of the db/db mice treated with placebo, LM06 at the dose of 50, 100 and 200 nmol/kg, and Semaglutide at the dose of 200 nmol/kg. All the above data shown as means ± SD, n=8. ***p<0.001 *vs.* placebo group, $^{\#}p$< 0.05 *vs.* Semaglutide group.

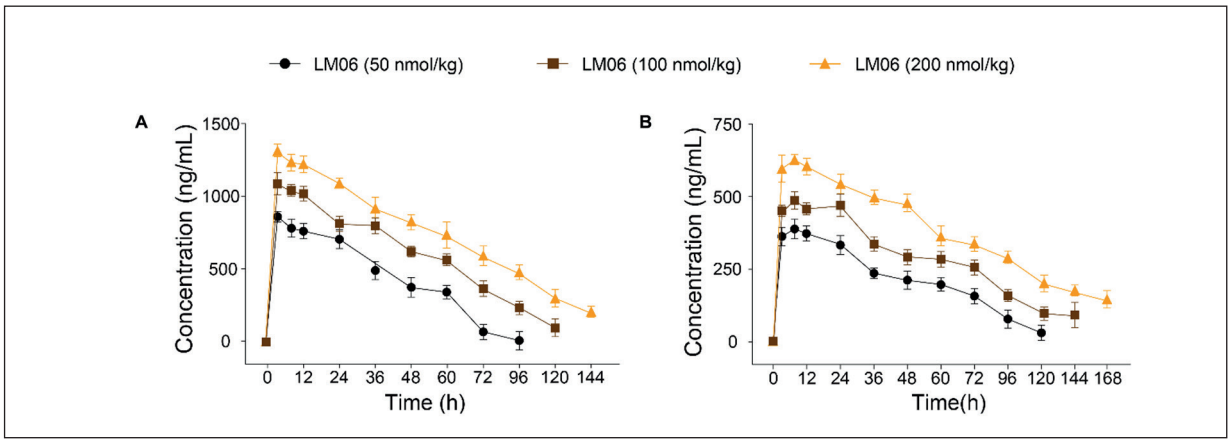

Figure 6. Pharmacokinetic tests of LM06 at different doses of 50, 100 and 200 nmol/kg in (**A**) SD rats (n=6) and (**B**) cynomolgus monkeys (n=3). All the results were showed as means ± SD.

low 8.35 mmol/L,as the normal state of rodent animals, in LM06 treated groups was ~23 h for 50 nmol/kg, ~35 h for 100 nmol/kg and ~67 h for 200 nmol/kg, respectively, while that of Semaglutide treated ones was only ~37 h. In addition, the $AUC_{0\text{-}120min}$ of LM06 at the dose of 200 nmol/kg was remarkably lower than that of the Semaglutide-treated group ($p<0.05$, Figure 5B). In general, LM06 exhibited enough potency to be developed as a long-acting antidiabetic peptide drug.

Pharmacokinetic Test

Pharmacokinetic properties of LM06 at 50, 100 and 200 nmol/kg were investigated in the SD rats and cynomolgus monkeys. Single subcutaneous injection of LM06 at all three doses induces the rapid absorption and the concentration peak within 4 and 8 hours in SD rat and cynomolgus monkey, respectively (Figure 6). As shown in Table III and IV, the average plasma half-life ($t_{1/2}$) of LM06 at the doses of 50, 100 and 200 nmol/kg were 53.19, 58.37 and 73.68 h in SD rats, and 56.40, 63.15 and 114.91 h in cynomolgus monkeys, respectively. Together with the results of multiple OGTTs and hypoglycemic duration test, LM06 was demonstrated with prolonged acute hypoglycemic activities due to the improved pharmacokinetic characters and exhibited potency as the one-weekly subcutaneous candidate for treating hyperglycemia.

Chronic Study

To further examine anti-diabetic as well potent anti-obesity effects, LM06 was subcutaneously administered twice a week for consecutive 8 weeks in db/db mice at three doses of 50, 100 and 200 nmol/kg using Semaglutide (200 nmol/kg) as positive control. As a result, LM06 at all three doses exhibited evident effects on body weight lowering accompanied by dose-dependent inhibition on food intake, while body weights of saline-treated db/db mice continued to increase during the entire experimental period (Figures 7A-B). Interestingly, chronic treatment of LM06 exhibited better efficacies on the body weight, as well as food intake control compared with those of Semaglutide treated mice at same dose (Figures 7A-B). In addition, a significant delay in gastric emptying

Table III. Pharmacokinetic parameters of LM06 in SD rats.

Parameters	LM06 (nmol/kg)		
	50	100	200
$AUC_{0\text{-}t}$ (ng/mL.h×10^4)	3.98 ± 0.36	6.64 ± 0.84	9.82 ± 0.59
C_{max} (ng/mL)	822.31 ± 64.35	1098.56 ± 106.21	1293.93 ± 197.55
$T_{1/2}$ (h)	53.19 ± 1.42	58.37 ± 4.51	73.68 ± 6.52

All values are presented as mean ± SD (n = 3).

Table IV. Pharmacokinetic parameters of LM06 in cynomolgus monkeys.

Parameters	LM06 (nmol/kg)		
	50	100	200
AUC0-t (ng/mL.h×104)	2.36 ± 0.15	3.69 ± 0.55	5.46 ± 0.36
Cmax (ng/mL)	380.26 ± 71.75	496.95± 64.84	626.16 ±53.47
T1/2 (h)	56.40 ± 2.71	63.15 ± 4.93	114.91 ±7.32

All values are presented as mean ± SD (n = 3).

was observed in LM06 treated groups, suggesting that the notable decrease in food intake is largely attributed to the delayed satiety in db/db mice (Figure 7C). Further analysis of body composition of db/db mice treated with all three doses of LM06 exhibited an evident decrease in the fat mass, but a slight but not significant reduction on the lean mass (Figure 7D). Similarly, weights of liver tissue, white fat tissue and subcutaneous tissue were significantly reduced after 8-week LM06 treatment (Figure 7E). In addition, OGTTs and insulin tolerance tests (ITTs)

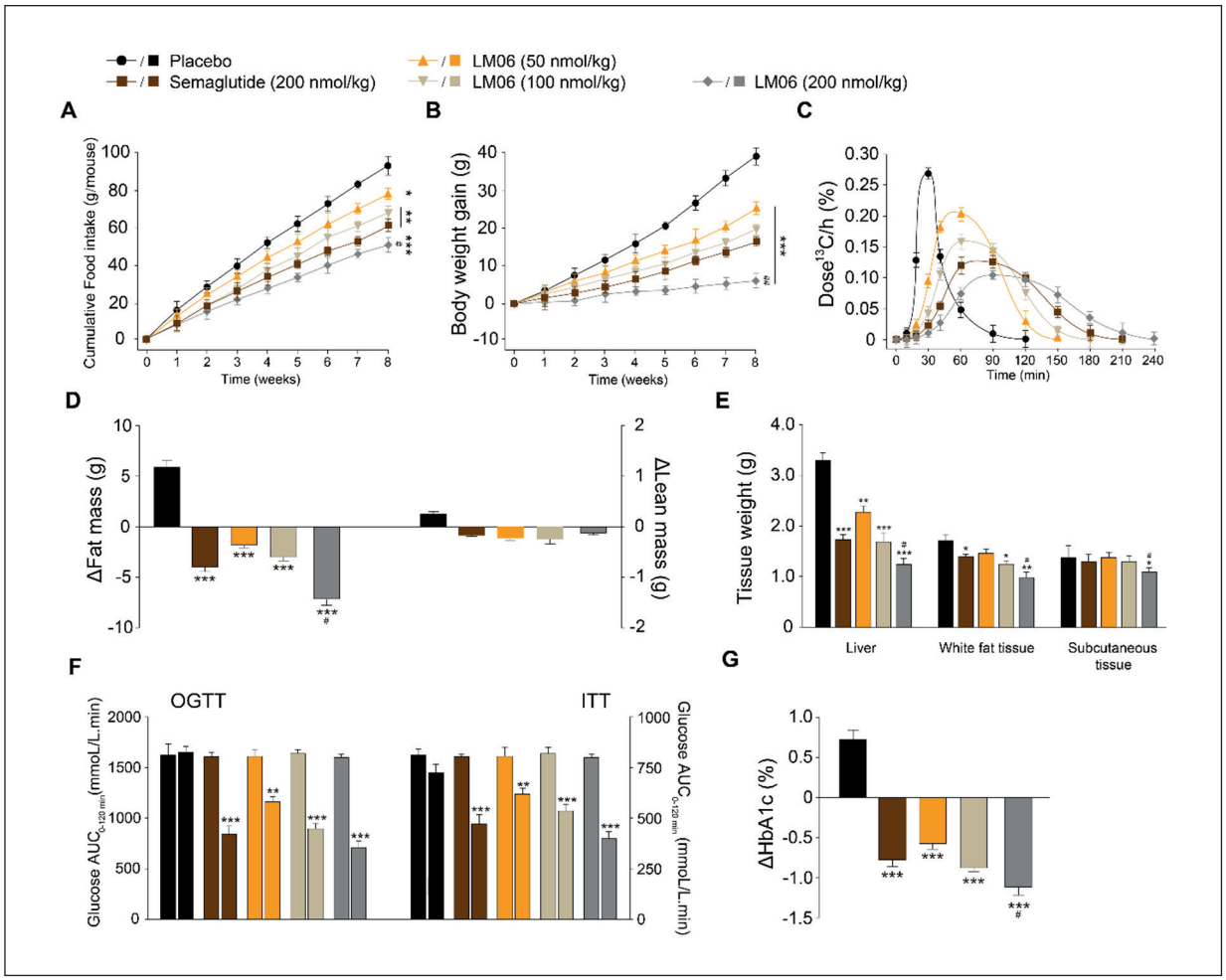

Figure 7. Chronic study of LM06 peptide in diabetic mice. Effect on (**A**) Cumulative food intake, (**B**) body weight gain, (**C**) gastric emptying, (**D**) body composition, (**E**) tissue weight, (**F**) $AUC_{0\text{-}120\ min}$ of OGTT and ITT, (**G**) HbA1c (%) in db/db mice. *p<0.05, **p<0.01, ***p<0.001 *vs.* placebo group, $^{\#}p$<0.05 *vs.* Semaglutide group. All above data are shown as means ± SD, n=8.

were conducted before and after 8-week efficacy experiment (Figure 7F). As we expected, different degrees of $AUC_{0\text{-}120min}$ value reductions were observed in LM06 treated groups in OGTT indicating a dose-dependent improvement on glucose tolerance in db/db mice. Consistently, the impaired insulin sensitivity observed in db/db mice was significantly improved with long-term LM06 treatment. In addition, treatments of LM06 at 50, 100 and 200 nmol/kg lead to significant decrease in Δ% HbA1c for 0.45%, 0.73% and 1.18%, respectively, which were all significant than that of the placebo treated ones (Figure 7G).

Moreover, the H&E staining was performed to assess long-term efficacies of LM06 on the pancreatic islets of the db/db mice. As the results showed in Figures 8A-G, significantly enhanced pancreatic area and more islets were observed in pancreas paraffin section from the diabetic mice treated with LM06 at three doses compared with that of the placebo treated group. Not only that, the improvement on area of pancreatic islet induced by LM06 was also significantly better than that of the Semaglutide treated ones at same dose of 200 nmol/kg. Furthermore, we conducted the histological analysis of WAT due to the enhanced fat loss of db/db mice which was involved in adipocyte differentiation and adipogenesis. As showed in Figure 9, the diabetic mice treated with LM06 at all three doses exhibited significantly smaller and more numerous adipocytes compared with that of the placebo-treated diabetic mice. In addition, the efficacies of LM06 on improving the adipocyte differentiation and adipogenesis were also better than Semaglutide at same dose.

Not only that, we further investigated the role of LM06 combined with low-intensity ultrasound in treating the refractory wounds of diabetic skin. As shown in Figure 10A, on the 10th day of treatment, the eschar surface area and wound area in the LM06 + low-intensity ultrasound group were significantly smaller than those in the LM06, low-intensity ultrasound alone and negative control groups. As shown in Figure 10B, the wound tissue healing rates of LM06 + low-intensity ultrasound on days 4 reached 100%, which were significantly higher than those of LM06, low-intensity ultrasound and negative control group, suggesting that LM06 combined with low-intensity ultrasound can effectively promote the recovery of refractory wounds in diabetic mice.

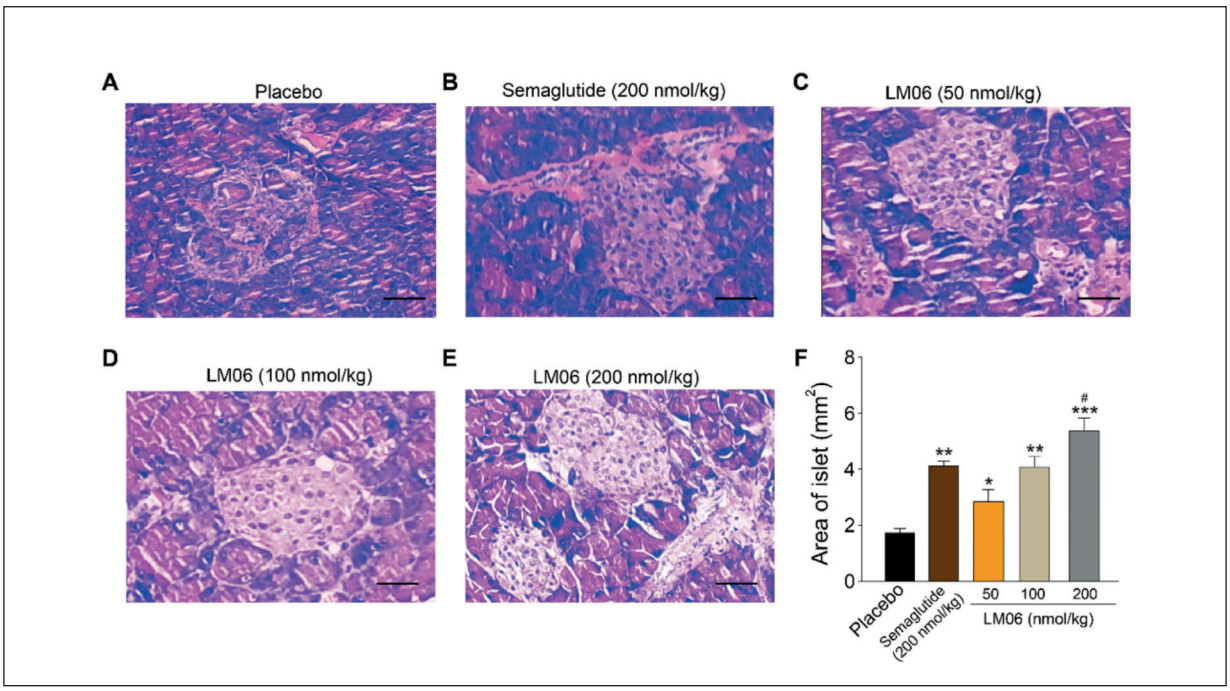

Figure 8. Effects of LM06 on the pancreatic islets in db/db mice. **A-E**, Representative images of histologic pancreatic islets (400×) from the db/db mice in five different groups. **F,** The area of pancreatic islets of the diabetic mice in each group. $^{**}p<0.01$, $^{***}p<0.001$ *vs.* placebo and $^{\#}p<0.05$ *vs.* Semaglutide group using one-way ANOVA. All the data were showed as mean ± SD (n=8).

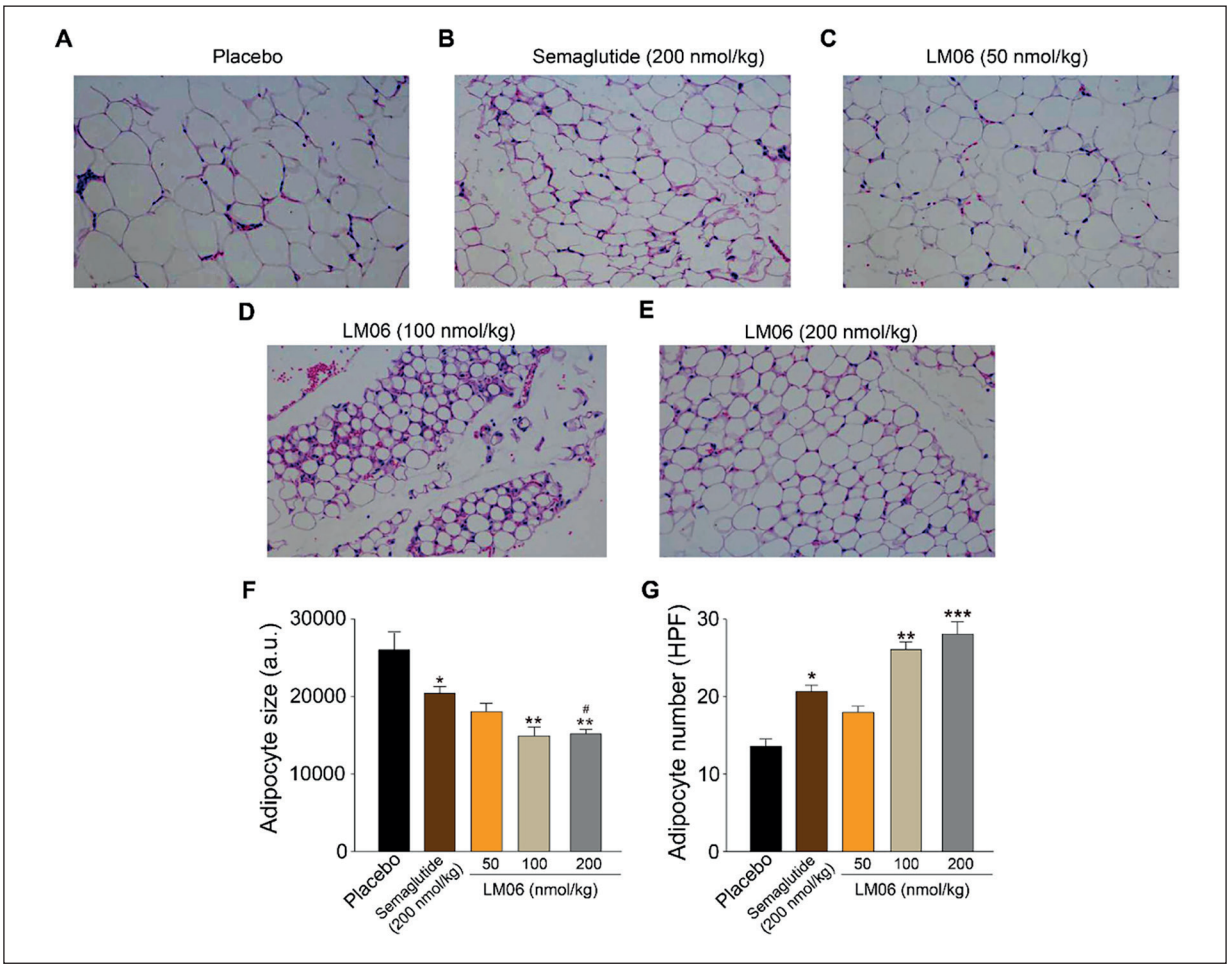

Figure 9. The histopathological evaluation of adipocytes from db/db mice. **A-E,** Representative microscopy images of the white adipocytes of db/db mice. The tissues section was stained by using HE method. Scale bar, 100 mm. (**F**) Adipocyte cell size and (**G**) adipocyte cell number per high-powered field (HPF) in db/db mice. *p<0.05, **p<0.01, ***p<0.001 vs. placebo group, $^{\#}p$<0.05 *vs.* Semaglutide group. All above data shown as means±SD, n=6.

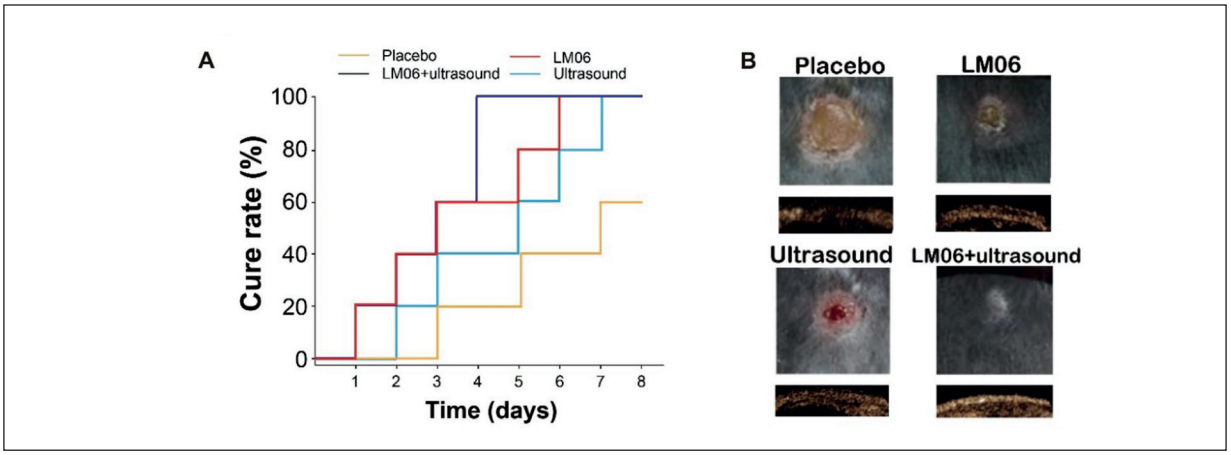

Figure 10. LM06 accelerates the skin wound closure in diabetic mice. The (**A**) wound closure rate-time curve and (**B**) images of the wound sites and ultrasonography.

Discussion

Recently, the incidence of diabetes mellitus, especially type 2 diabetes mellitus (T2DM), has been gradually increasing[26]. According to WHO prediction, the number of patients with diabetes mellitus will reach 300 million worldwide by 2025, and more than 90% of them are T2DM which has become the third chronic non-transmissible disease that seriously endangers the health of the people[27,28]. At present, incretin-based peptides have become one of the research hotspots of T2DM treatment because of many physical effects such as reducing glucagon level, stimulating pancreatic island B cell proliferation and differentiation, promoting pancreatic island secretion, reducing gastric evacuation space velocity rate, and increasing satiety sensation[29,30].

Oxyntomodulin (OXM) is a peptide kinin secreted by L cells of the small intestinal mucosa consisting of 37 amino acid residues[31]. OXM could stimulate both GLP-1R and GcgR, and holds biological functions such as inhibiting gastric acid secretion, reducing feed intake, increasing energy expenditure, reducing body weight, and promoting insulin secretion[8]. However, the clinical application of the OXM-based molecules was hampered due to the limited bioavailability which was induced by the short *in vivo* $t_{1/2}$[14,32]. After replacing the serine (Ser) at position 2 of OXM with dextraserine (D-Ser), it becomes a Ser^2-OXM which could be protected from degradation by dipeptidase IV (DPP-IV) to increase its *in vivo* half-life[24,33]. In addition, we designed and evaluated a series of novel HSA-binding domain, G148-ABD, showing outstanding affinity with HSA between femtomolar to picomole level according to previously reports[18].

In present study, we fused the above mentioned modified OXM analog, ($D\text{-}Ser^2$) OXM, to different helixes of G148-ABD via a thrombin-cleavable site (FNKP) to generate seven OXM derivatives with enhanced resistance to the DPP-IV degradation (Figure 1). All seven peptides as native OXM were all synthesized with purities more than 98%. Subsequently, the CHO cells stably expressing GcgR or GLP-1R were utilized to assess the potencies of LM01-LM07 on activations of GLP-1R and GcgR. Most of the seven LM peptides, except LM04 and LM07, retained the similar activation potencies for GcgR and GLP-1R as native OXM (Table II) indicating the steric hindrance effects induced by the excessively complex helical structure may affect the potency on receptor activation. Hence, further albumin binding affinity test proved those ones contained helix 2 or helix 3 or both held the higher binding affinities for albumin, such as LM02, LM03 and LM06.

We further observed whether the thrombin could stably digest and release the $D\text{-}Ser^2$-OXM from LM peptides in a moderate rate. There the thrombin cleavage assay of LM02, LM03 and LM06 was performed in the monkey serum *in vitro*. As the results showed in Figure 2, the intact LM peptides, helix-thrombin cleavable site (FNPK) as well as released $D\text{-}Ser^2$-OXM were all could be detected at 12 h and 72 h using the method of LC-MS/MS in mixture of the thrombin cleavage reaction. Interestingly, the concentration of released $D\text{-}Ser^2$-OXM in LM06 group was significantly higher than LM02 and LM03 at 96 h. Therefore, LM06 peptide was selected as the candidate to conduct the acute and long-term efficacy evaluation in model rodent animals.

Two kinds of knock-out ($GLP\text{-}1^{-/-}$, $GcgR^{-/-}$) mice and WT mice were utilized in the OGTT. As the results showed in Figure 3, the AUC of insulin levels of LM06 treated WT mice at three doses were all significantly higher than that of the placebo treated mice. Meanwhile, these changes on insulin level attributed to the significant reductions on BGLs. However, treatment of LM06 at 100 and 200 nmol/kg in $GLP\text{-}1R^{-/-}$ mice increased the BGLs due to the GcgR activation alone. Moreover, in $GcgR^{-/-}$ mice, LM06 treatment caused a similar insulin level increase and glucose level reduction as those in WT mice. All these results definitively demonstrated the insulinotropic and hypoglycemic activities of LM06 at all three doses which were almost relied on GLP-1R activation. Further multiple OGTTs and hyperglycemic duration assay were performed to assess the prolonged efficacies of LM06 at three doses in non-fasted and fasted db/db mice, respectively. As shown in Figure 4, LM06 treatment (50, 100 and 200 nmol/kg) dose-dependently reduced the BGLs of db/db mice in all three OGTTs. Moreover, LM06 induced a greater extent on $AUC_{0\text{-}120min}$ value reduction in third round of OGTT compared to Semaglutide at same dose ($p<0.05$). Combined with similar results showed in the hyperglycemic duration test, LM06 held the better glucoregulatory effect and hyperglycemic duration than Semaglutide, the best incretin-based antidiabetic drug, and exhibited enough potency to be a long-acting antidiabetic protein drug.

To comprehensively investigate the potency of LM06 on anti-obesity and anti-diabetic effects, we conducted a consecutive 8-week efficacy evaluation in the db/db mice, a classic diabetic and obesity rodent model animal. All three doses of LM06 exhibited dose-dependent inhibition on the body weight gain as well as the food intake (Figures 8A-B) which were better than Semaglutide at same dose. Significant delay in gastric emptying was observed in Figure 8C, which largely induced the reduction in food intake. Further body composition analysis of LM06 treated mice exhibited significant decreased fat mass in all three doses (Figure 8D). Similarly, weights of liver tissue, WAT and subcutaneous tissue were significantly reduced after 8-week LM06 treatment (Figure 8E). Above results preliminarily proved that the promising weight loss induced by chronic treatment of LM06 is largely due to the reduction of the 'bad fat tissue' as well as the decreased appetite. Further OGTTs as well insulin tolerance tests indicated a dose-dependent improvement on glucose tolerance and insulin sensitivity in db/db mice by 8-week treatment of LM06. Consistently, chronic treatment of LM06 at three doses all lead to evident decrease in Δ%HbA1c (Figure 7G) indicating the better long-term improvement on blood glucose level.

Further H&E staining detection of pancreatic islets and WAT were performed to assess long-term efficacies of LM06 on the db/db mice. The results showed in Figures 8-9 both demonstrated the enhanced improvement of LM06 on both islet and WAT which were also both significantly better than those of the placebo-treated ones. These data collectively suggested that in diabetic mice treated LM06, the adipose tissue mass increases cell number rather than via increasing adipocyte size which was correlated with the accumulation of pro-inflammatory macrophages into adipose tissue contributing to insulin resistance, an important risk factor for diabetes. Not only that, we further demonstrated that LM06 combined with low-intensity ultrasound had a very significant effect on refractory diabetic skin wounds and could effectively promote wound healing rate compared with the control group (Figure 10).

Above results directly demonstrated the high therapeutic potential of LM06 for the treatment of T2DM and obesity, and these findings open new avenues for the further development of new drugs. With this strategy in hand, it should be possible to expand the application range of peptide therapeutics from the current mostly short-lived agents that act mainly as receptor agonists to long-acting peptide drugs which activated multiple receptors.

Conclusions

In summary, our research on sustained release of D-Ser^2-OXM from LM06, a dual GLP-1R and GcgR agonist with outstanding albumin binding domain and thrombin cleavable-site, provides promise for the not only treatment of T2DM and with promote the wound healing low-intensity ultrasound, but also can be applied in other peptides or proteins for these diseases.

Conflict of Interest

The Authors declare that they have no conflict of interests.

Acknowledgements

This study was supported by the internal research fund of Zhejiang University.

References

1) Arulmozhi DK, Portha B. GLP-1 based therapy for type 2 diabetes. Eur J Pharm Sci 2006; 28: 96-108
2) Tielmans A, Laloi-Michelin M, Coupaye M, Virally M, Meas T, Guillausseau PJ. Drug treatment of type 2 diabetes. Presse Méd 2007; 36: 269.
3) Ullah N, Hafeez K, Farooq S, Batool A, Aslam N, Hussain M, Ahmad S. Anti-diabetes and anti-obesity: A meta-analysis of different compounds. Asian Pac J Trop Med 2016; 6: 749-756.
4) Finan B, Yang B, Ottaway N, Smiley D, Ma T, Clemmensen C, Chabenne J, Zhang L, Habegger K, Fischer K, Campbell J, Sandoval D, Seeley R, Bleicher K, Uhles S, Riboulet W, Funk J, Hertel C, Belli S, Tschöp M. A rationally designed monomeric peptide triagonist corrects obesity and diabetes in rodents. Nat Med 2014; 21: 27-36.
5). Henderson SJ, Konkar A, Hornigold DC, Trevaskis JL, Jackson R, Fritsch Fredin M, Jansson-Lofmark R, Naylor J, Rossi A, Bednarek MA, Bhagroo N, Salari H, Will S, Oldham S, Hansen G, Feigh M, Klein T, Grimsby J, Maguire S, Jermutus L, Rondinone CM, Coghlan MP. Robust anti-obesity and metabolic effects of a dual GLP-1/glucagon receptor peptide agonist in rodents and non-human primates. Diabetes Obes Metab 2016; 18: 1176-1190.
6) Lee, Oh. adipose tissue-derived signatures for obesity and type 2 diabetes: adipokines, batokines and MicroRNAs. J Clin Med 2019; 8: 854.

7) Lofthouse M. Oxyntomodulin—a novel treatment for human obesity. Nat Clin Pract Endoc 2005; 1: 9-9

8) Pimentel GD, Mota JF, Oyama LM. Oxyntomodulin and obesity. Revista De Nutrio 2009; 22: 727-737

9) Heppner KM, Diego PT. GLP-1 based therapeutics: simultaneously combating T2DM and obesity. Front Neurosci 2015; 9: 92

10) Li Y, Huang TH-W, Yamahara J. Salacia root, a unique Ayurvedic medicine, meets multiple targets in diabetes and obesity. Life Sci 2008; 82: 1045-1049

11) Druce MR, Minnion JS, Field BCT, Patel SR, Shillito JC, Michael T, Beale KEL, Murphy KG, Ghatei MA, Bloom SR. Investigation of structure-activity relationships of oxyntomodulin (Oxm) using Oxm analogs. Endocrinology 2008; 150: 1712-1722

12) Pocai, Alessandro. Action and therapeutic potential of oxyntomodulin. Mol Metab 2014; 3: 241-251

13) Muppidi A, Zou H, Yang P, Chao E, Sherwood L, Nunez V, Woods A, Schultz P, Lin Q, Shen W. Design of potent and proteolytically stable oxyntomodulin analogs. ACS Chem Biol 2016; 11: 324-328

14) Santoprete A, Capitò E, Carrington PE, Pocai A, Pessi A. DPP-IV-resistant, long-acting oxyntomodulin derivatives. J Pept Sci 2011; 17: 270-280

15) Wynne K, Field BC, Bloom SR. The mechanism of action for oxyntomodulin in the regulation of obesity. Curr Opin Investig Drugs 2010; 11: 1151-1157

16) Ishima Y, Maruyama T. Human serum albumin as carrier in drug delivery systems. Yakugaku Zasshi Journal of the Pharmaceutical Society of Japan 2016; 136: 39-47

17) Larsen MT, Kuhlmann M, Hvam ML, Howard KA. Albumin-based drug delivery: harnessing nature to cure disease. Mol Cell Ther 2016; 4: 3

18) Ahmad JN, Li J, Biedermannová L, Kucha M, Sípová H, Semerádtová A, Cerný J, Petroková H, Mikulecky P, Polínek J. Novel high-affinity binders of human interferon gamma derived from albumin-binding domain of protein G. Proteins 2012; 80: 774-789

19) Siebring-Van Olst E, Vermeulen C, De Menezes RX, Howell M, Smit EF, Van Beusechem VW. Affordable luciferase reporter assay for cell-based high-throughput screening. J Biomol Screen 2013; 18: 453-461

20) Wang TJ, Li J, Liang LJ, Zhong M, Chen XH, Kai shun BI. Determination of trillin in mouse plasma by LC-MS/MS method and pharmacokinetic study. Chinese Journal of Pharmaceutical Analysis 2007; 27: 984-988

21) Carrara MA, Batista MR, Saruhashi TR, Felisberto-Junior AM, Guilhermetti M, Bazotte RB. Coexistence of insulin resistance and increased glucose tolerance in pregnant rats: a physiological mechanism for glucose maintenance. Life Sci 2012; 90: 831-837.

22) Bluck LJC, Jackson SJ, Vlasakakis G, Mander A. Bayesian hierarchical methods to interpret the 13c-octanoic acid breath test for gastric emptying. Digestion 2010; 83: 96-107

23) Christiaens V, Van Hul M, Lijnen HR, Scroyen I. CD36 promotes adipocyte differentiation and adipogenesis. Biochim Biophys Acta 2012; 1820: 949-956

24) Kerr BD, Flatt PR, Gault VA. (D-Ser2)Oxm[mPEG-PAL]: a novel chemically modified analogue of oxyntomodulin with antihyperglycaemic, insulinotropic and anorexigenic actions. Biochem Pharmacol 2010; 80: 1727-1735.

25) Li H, Ma Y, Chen Y, Sang Y, Su Z. A Protease-based strategy for the controlled release of therapeutic peptides. Angew Chem 2010; 49: 4930-4933.

26) Rodbard HW. The clinical impact of GLP-1 receptor agonists in type 2 diabetes: focus on the long-acting analogs. Diabetes Technol Ther 2018; 20: S233-S241.

27) Yadollahpour A, Hosseini SA, Tabasi M, Shirali S, Saki S. Viruses and diabetes: a long history. Int J Pharm Res Allied Sci 2016; 5: 258.

28) Wilding, H. JP. The importance of weight management in type 2 diabetes mellitus. Int J Clin Pract 2014; 68: 682-691.

29) Ali S, Lamont BJ, Charron MJ, Drucker DJ. Dual elimination of the glucagon and GLP-1 receptors in mice reveals plasticity in the incretin axis. J Clin Invest 2011; 121: 1917-1929.

30) Drucker DJ, Nauck MA. The incretin system: glucagon-like peptide-1 receptor agonists and dipeptidyl peptidase-4 inhibitors in type 2 diabetes. Lancet 2006; 368: 1696-1705.

31) Druce MR, Bloom PSR. Oxyntomodulin. Treat Endocrinol 2006; 5: 265-272.

32) Bianchi E, Carrington PE, Ingallinella P, Finotto M, Santoprete A, Petrov A, Eiermann G, Kosinski J, Marsh DJ, Pocai A. A PEGylated analog of the gut hormone oxyntomodulin with long-lasting antihyperglycemic, insulinotropic and anorexigenic activity. Biorg Med Chem 2013; 21: 7064-7073.

33) Pathak NM, Pathak V, Lynch AM, Irwin N, Gault VA, Flatt PR. Stable oxyntomodulin analogues exert positive effects on hippocampal neurogenesis and gene expression as well as improving glucose homeostasis in high fat fed mice. Mol Cell Endocrinol 2015; 412: 95-103.